

Elastic Full Wavefield Migration using Shuey's approximation

Hoogerbrugge, L.; van Dongen, K.; Verschuur, E.

DOI

[10.3997/2214-4609.2024101641](https://doi.org/10.3997/2214-4609.2024101641)

Publication date

2024

Document Version

Final published version

Citation (APA)

Hoogerbrugge, L., van Dongen, K., & Verschuur, E. (2024). *Elastic Full Wavefield Migration using Shuey's approximation*. Paper presented at 85th EAGE Annual Conference & Exhibition 2024, Oslo, Lillestrøm, Norway. <https://doi.org/10.3997/2214-4609.2024101641>

Important note

To cite this publication, please use the final published version (if applicable). Please check the document version above.

Copyright

Other than for strictly personal use, it is not permitted to download, forward or distribute the text or part of it, without the consent of the author(s) and/or copyright holder(s), unless the work is under an open content license such as Creative Commons.

Takedown policy

Please contact us and provide details if you believe this document breaches copyrights. We will remove access to the work immediately and investigate your claim.

Green Open Access added to TU Delft Institutional Repository

'You share, we take care!' - Taverne project

<https://www.openaccess.nl/en/you-share-we-take-care>

Otherwise as indicated in the copyright section: the publisher is the copyright holder of this work and the author uses the Dutch legislation to make this work public.

Elastic Full Wavefield Migration using Shuey's approximation

L. Hoogerbrugge¹, K. Van Dongen¹, E. Verschuur¹

¹ TU Delft

Summary

The phenomenon of wave conversions, where acoustic, pressure (P) waves are converted to elastic, shear (S) waves is commonly disregarded in seismic imaging, which can lead to lower-quality images in regions with strong reflectors. While a number of methods exist which do take wave conversions into account, most deal with P- and S-waves separately, rather than in using a single, unified, framework. Elastic Full-Waveform Inversion (FWI), on the other hand, which does offer a unified framework for all elastic effects, is prohibitively computationally expensive in many cases.

We present an alternative approach by extending Full Wavefield Migration (FWM) to account for wave conversions. Full Wavefield Migration describes seismic data in terms of convolutional propagation and reflection operators in the space-frequency domain. By applying these operators recursively, multi-scattering data can be modelled and inverted. Using Shuey's approximation to constrain the number of parameters necessary to describe the full, elastic, reflection and transmission operators, we present an elastic FWM algorithm which accounts for wave conversions.

The resulting algorithm is tested on a synthetic model to give a proof of concept. The results show that the proposed extension can model wave conversions accurately and yields better inversion results than applying conventional, acoustic FWM.

Elastic Full Wavefield Migration using Shuey's approximation

While the earth is an elastic medium in reality, most conventional migration methods treat it as an acoustic medium in practice. While this approach has produced good results, it disregards the possibility of wave conversions, where pressure (P) waves are converted into shear (S) waves and vice versa. In areas with high contrasts, such as around salt bodies (Jones and Davison, 2014), and in areas containing so-called 'gas clouds' (Ensley, 1984), converted waves play a large role, and accounting for them can increase the quality of the resulting migration images.

In recent years, this fact has been recognized, and multiple methods have been proposed to include converted waves in the migration process, with the 'holy grail' being elastic Full-Waveform Inversion (FWI) (Virieux and Operto, 2009). However, elastic FWI is an exceptionally computationally expensive technique, making it impractical in many cases. In this work, we present an alternative method by extending Full-Wavefield Migration (FWM) (Berkhout, 2014b) to take converted waves into account.

The potential to incorporate wave conversions into FWM has been recognized from the start (Berkhout, 2014c). However, the fact that one needs to invert each of the 16 possible reflection and transmission coefficients separately for every angle has been a challenge in practice, as it leads to a significant over-parametrisation. To avoid this issue, and to avoid the non-linearity present in the full Zoeppritz reflection and transmission coefficients, we use Shuey's approximation (Shuey, 1985) to link the different angles together. In this way, we introduce a robust elastic FWM algorithm that accounts for wave conversions.

Theory

Following the approach outlined by Berkhout (2014a), we begin by splitting the P - and S -wavefields into up- and downgoing components. Examining the wavefield at the locations (x_i, z_n^-) and (x_i, z_n^+) , located right above and below an interface at $z = z_n$, respectively, we write

$$p_{P/S}(x_i, z_n^\pm) = p_{P/S}^\mp(x_i, z_n^\pm) + q_{P/S}^\pm(x_i, z_n^\pm), \quad (1)$$

where the superscripts $-$ and $+$ denote up- and downgoing waves, p and q denote waves traveling towards and away from the interface, and the subscripts P and S denote P - and S -wavefields, respectively. Also note the angular frequency ω , as we will work in the temporal Fourier domain throughout this work.

Next, we describe the relationship between wavefields above and below the interface. Assuming a rectangular grid of N_x evenly spaced points in the lateral direction and N_z points in the depth direction, we introduce the vectors $\mathbf{p}_{P/S}^\pm(z_n)$ of length N_x , with elements $\mathbf{p}_{P/S}^\pm(z_n)|_i = p_{P/S}^\pm(x_i, z_n)$, with a similar definition for $\mathbf{q}_{P/S}^\pm(z_n)$. Using the formulation of Berkhout (2014a), we use convolutional reflection and transmission operators, denoted as \mathbf{R}^\pm and \mathbf{T}^\pm , respectively, to write

$$\begin{pmatrix} \mathbf{q}_P^+(z_n^+) \\ \mathbf{q}_S^+(z_n^+) \end{pmatrix} = \begin{pmatrix} \mathbf{R}_{PP}^\cap & \mathbf{R}_{PS}^\cap \\ \mathbf{R}_{SP}^\cap & \mathbf{R}_{SS}^\cap \end{pmatrix} \begin{pmatrix} \mathbf{p}_P^-(z_n^+) \\ \mathbf{p}_S^-(z_n^+) \end{pmatrix} + \begin{pmatrix} \mathbf{T}_{PP}^+ & \mathbf{T}_{PS}^+ \\ \mathbf{T}_{SP}^+ & \mathbf{T}_{SS}^+ \end{pmatrix} \begin{pmatrix} \mathbf{p}_P^+(z_n^-) \\ \mathbf{p}_S^+(z_n^-) \end{pmatrix}, \quad (2)$$

$$\begin{pmatrix} \mathbf{q}_P^-(z_n^-) \\ \mathbf{q}_S^-(z_n^-) \end{pmatrix} = \begin{pmatrix} \mathbf{R}_{PP}^\cup & \mathbf{R}_{PS}^\cup \\ \mathbf{R}_{SP}^\cup & \mathbf{R}_{SS}^\cup \end{pmatrix} \begin{pmatrix} \mathbf{p}_P^+(z_n^-) \\ \mathbf{p}_S^+(z_n^-) \end{pmatrix} + \begin{pmatrix} \mathbf{T}_{PP}^- & \mathbf{T}_{PS}^- \\ \mathbf{T}_{SP}^- & \mathbf{T}_{SS}^- \end{pmatrix} \begin{pmatrix} \mathbf{p}_P^-(z_n^+) \\ \mathbf{p}_S^-(z_n^+) \end{pmatrix}, \quad (3)$$

where \mathbf{R}^\pm and \mathbf{T}^\pm are matrices of size $N_x \times N_x$ which relate the wavefields above and below the interface. Note that we have dropped the z_n -dependence of these matrices for ease of legibility.

Next, we examine the relationship between the wavefields at different depth levels z_n . To do this, we introduce a set of propagation operators $\mathbf{W}_{P/S}(z_{n\pm 1}, z_n)$ such that

$$\begin{pmatrix} \mathbf{p}_P^+(z_{n+1}^-) \\ \mathbf{p}_S^+(z_{n+1}^-) \end{pmatrix} = \begin{pmatrix} \mathbf{W}_P(z_{n+1}, z_n) & \mathbf{0} \\ \mathbf{0} & \mathbf{W}_S(z_{n+1}, z_n) \end{pmatrix} \begin{pmatrix} \mathbf{q}_P^+(z_n^+) \\ \mathbf{q}_S^+(z_n^+) \end{pmatrix}, \quad (4)$$

$$\begin{pmatrix} \mathbf{p}_P^-(z_{n-1}^+) \\ \mathbf{p}_S^-(z_{n-1}^+) \end{pmatrix} = \begin{pmatrix} \mathbf{W}_P(z_{n-1}, z_n) & \mathbf{0} \\ \mathbf{0} & \mathbf{W}_S(z_{n-1}, z_n) \end{pmatrix} \begin{pmatrix} \mathbf{q}_P^-(z_n^-) \\ \mathbf{q}_S^-(z_n^-) \end{pmatrix}, \quad (5)$$

with $\mathbf{W}_{P/S}(z_{n\pm 1}, z_n)$ matrices of size $N_x \times N_x$ which describe the propagation of waves between the different depth levels, and $\mathbf{0}$ the zero matrix of size $N_x \times N_x$. These propagation operators are described in detail in Berkhout (2014a).

We now examine the reflection and transmission operators \mathbf{R}^{\cup} and \mathbf{T}^{\cup} in more detail. To avoid the non-linearity of the full Zoeppritz equations we use Shuey's approximation. For a flat reflector, Shuey's approximation for the PP -reflection coefficient is given by (Shuey, 1985)

$$R_{PP}^{\cup}(\theta) \approx \frac{1}{2} \left(\frac{\Delta V_P}{V_P} + \frac{\Delta \rho}{\rho} \right) + \sin^2(\theta) \left(\frac{1}{2} \frac{\Delta V_P}{V_P} - 2 \left(\frac{V_S}{V_P} \right)^2 \left(\frac{\Delta \rho}{\rho} + 2 \frac{\Delta V_S}{V_S} \right) \right), \quad (6)$$

with V_P and V_S the P - and S -wave velocities, ρ the density of mass and θ the angle of incidence of the incoming wave. Rewriting equation 6 using the notation of equations 2 and 3 gives

$$\mathbf{R}_{PP}^{\cup} = \frac{\Delta x}{2} (\mathbf{C}_P + \mathbf{C}_\rho) + \mathbf{S}_{\theta,2} \Delta x \left(\frac{1}{2} \mathbf{C}_P - 2 \hat{\mathbf{V}}^2 (\mathbf{C}_\rho + 2 \mathbf{C}_S) \right). \quad (7)$$

In equation 7 we have introduced the contrast matrix \mathbf{C}_P , which is a diagonal matrix with elements $\mathbf{C}_P(z_n)|_{ii} = C_P(x_i, z_n) = \Delta V_P(x_i, z_n) / V_P(x_i, z_n)$, with similar definitions for $\mathbf{C}_S(z_n)$ and $\mathbf{C}_\rho(z_n)$. We have also introduced the velocity ratio matrix $\hat{\mathbf{V}}(z_n)$, which is a diagonal matrix with elements $\hat{\mathbf{V}}(z_n)|_{ii} = V_S(x_i, z_n) / V_P(x_i, z_n)$. Finally, we have introduced the operators $\mathbf{S}_{\theta,m}(z_n)$, which are defined as

$$\mathbf{S}_{\theta,m}(z_n)|_{ij} = \mathcal{F}^{-1} \left\{ \sin^m(\theta_n^i) \right\} \Big|_{x=x_j} = \mathcal{F}^{-1} \left\{ \left(\frac{V_P(x_i, z_n) k_x}{\omega} \right)^m \right\} \Big|_{x=x_j}, \quad (8)$$

where \mathcal{F}^{-1} is the inverse (spatial) Fourier transform in the lateral direction. Extending the notation introduced above to the full reflection and transmission operators, we write

$$\mathbf{R}^{\cup/\cap}(z_n) = \pm \mathbf{R}_0(z_n) \pm \mathbf{R}_\theta(z_n), \quad (9)$$

where $\mathbf{R}_0(z_n)$ represents the zero-offset reflectivity, while $\mathbf{R}_\theta(z_n)$ represents the angle-dependent reflectivity. These operators are given by

$$\mathbf{R}_0(z_n) = \begin{pmatrix} \frac{\Delta x}{2} (\mathbf{C}_P + \mathbf{C}_\rho) & 0 \\ 0 & -\frac{\Delta x}{2} (\mathbf{C}_S + \mathbf{C}_\rho) \end{pmatrix}, \quad (10)$$

$$\mathbf{R}_\theta(z_n) = \begin{pmatrix} \frac{\Delta x}{2} (\mathbf{C}_P - 4 \hat{\mathbf{V}}^2 \mathbf{D}) \mathbf{S}_{\theta,2}(z_n) & -\frac{\Delta x}{2} (\mathbf{C}_\rho + 2 \hat{\mathbf{V}} \mathbf{D}) \hat{\mathbf{V}} \mathbf{S}_{\theta,1}(z_n) \\ -\frac{\Delta x}{2} (\mathbf{C}_\rho + 2 \hat{\mathbf{V}} \mathbf{D}) \mathbf{S}_{\theta,1}(z_n) & -\frac{\Delta x}{2} (\mathbf{C}_S - 4 \mathbf{D}) \hat{\mathbf{V}}^2 \mathbf{S}_{\theta,2}(z_n) \end{pmatrix}, \quad (11)$$

where we have introduced $\mathbf{D} = \mathbf{C}_\rho + 2 \mathbf{C}_S$. In a similar way, we write the transmission operators as

$$\mathbf{T}^{\pm}(z_n) = \mathbf{I} \pm \mathbf{T}_0(z_n) \pm \mathbf{T}_\theta(z_n), \quad (12)$$

with

$$\mathbf{T}_0(z_n) = \begin{pmatrix} -\frac{\Delta x}{2} (\mathbf{C}_P + \mathbf{C}_\rho) & 0 \\ 0 & -\frac{\Delta x}{2} (\mathbf{C}_S + \mathbf{C}_\rho) \end{pmatrix}, \quad (13)$$

$$\mathbf{T}_\theta(z_n) = \begin{pmatrix} \frac{\Delta x}{2} \mathbf{C}_P \mathbf{S}_{\theta,2}(z_n) & -\frac{\Delta x}{2} (\mathbf{C}_\rho - 2 \hat{\mathbf{V}} \mathbf{D}) \hat{\mathbf{V}} \mathbf{S}_{\theta,1}(z_n) \\ \frac{\Delta x}{2} (\mathbf{C}_\rho - 2 \hat{\mathbf{V}} \mathbf{D}) \mathbf{S}_{\theta,1}(z_n) & \frac{\Delta x}{2} \mathbf{C}_S \hat{\mathbf{V}}^2 \mathbf{S}_{\theta,2}(z_n) \end{pmatrix}. \quad (14)$$

Using the building blocks of equations 2 - 5, we can now formulate a forward modelling algorithm, which can be seen as the elastic extension of Full-Wavefield Modelling (FWMoD) (Berkhout, 2014a). Assuming a known source wavefield \mathbf{s}_0 at the surface, one can recursively apply equations 2 and 4 to model the downgoing wavefield at each depth level, after which equations 3 and 5 can be used to find the corresponding upgoing wavefield. By repeating this process multiple times, multiple scattering events can be taken into account. This process is illustrated in algorithm 1.

Algorithm 1: Elastic Full-Wavefield Modelling

Result: $\mathbf{p}^{+,M}(z_n)$ and $\mathbf{p}^{-,M}(z_n)$ for all z_n .

Input: \mathbf{s}_0

```

1 Set  $\mathbf{p}^{-,0}(z_n) = \mathbf{0}$ ;
2 for  $m = 1 : M$  do
3   Set  $\mathbf{p}^{+,m}(z_0) = \mathbf{s}_0$ ;
4   for  $n = 0 : N_z - 1$  do
5      $\mathbf{q}^{+,m}(z_n) = \mathbf{T}^+(z_n)\mathbf{p}^{+,m}(z_n) + \mathbf{R}^\cap(z_n)\mathbf{p}^{-,m-1}(z_n)$ ;
6      $\mathbf{p}^{+,m}(z_{n+1}) = \mathbf{W}(z_{n+1}, z_n)\mathbf{q}^{+,m}(z_n)$ ;
7   end
8   Set  $\mathbf{p}^{-,m}(z_{N_z}) = \mathbf{0}$ ;
9   for  $n = N_z : 1$  do
10     $\mathbf{q}^{-,m}(z_n) = \mathbf{T}^-(z_n)\mathbf{p}^{-,m}(z_n) + \mathbf{R}^\cup(z_n)\mathbf{p}^{+,m}(z_n)$ ;
11     $\mathbf{p}^{-,m}(z_{n-1}) = \mathbf{W}(z_{n-1}, z_n)\mathbf{q}^{-,m}(z_n)$ ;
12  end
13 end
  
```

In a similar way, a migration algorithm can be set up based on this framework. Following Berkhout (2014b), we define the objective function

$$J = \frac{1}{2} \sum_{i=1}^{N_\omega} \sum_{j=1}^{N_s} \|\mathbf{d}(z_0, s_j, \omega_i) - \mathbf{p}^{-,M}(z_0, s_j, \omega_i, C_P, C_S, C_\rho)\|^2, \quad (15)$$

where $\mathbf{d}(z_0, s_j, \omega_i)$ is the known data recorded at the surface and $\mathbf{p}^{-,M}(z_0, s_j, \omega_i, C_P, C_S, C_\rho)$ is the forward modelled wavefield up to scattering order M . Note that we have explicitly written the dependence of these wavefields on the source location s_j and the frequency ω_i . Applying a gradient descent scheme with respect to the contrasts $C_P(x, z)$, $C_S(x, z)$ and $C_\rho(x, z)$, one can within the medium.

Results

We apply the method described above to a synthetic, layered model, shown in figures 1a) - 1c). The model chosen features a strong reflector in the centre, representing a highly simplified salt-body model, which are known to generate strong converted-wave effects. Synthetic data was generated using a Kennett modelling scheme (Kennett, 1984) with a Ricker wavelet source with a peak frequency of 17 Hz. Migration was performed on a grid of $N_x = 201$ by $N_z = 301$ points with a spacing of $\Delta x = 10$ m and $\Delta z = 5$ m. The results of the migration process are shown in figure 1d) - 1f).

Examining these results, we see that applying elastic FWM leads to a significant uplift when compared to conventional, acoustic, FWM. Specifically, we see an improved continuity of the layers when applying elastic FWM and an improved recovery of the amplitudes of the reflectors. While these results are promising, we see that the result of figure 1e) still contains an unwanted, background, ‘smearing’ effect. This is most likely caused by the fact that Shuey’s approximation is not accurate for large offsets, leading to confusion for large angles of incidence. To improve this behaviour, we recommend investigating alternative formulations of the reflection and transmission coefficients, which may be more accurate for large angles. Alternatively, large angles can be filtering out from the input data to reduce these effects.

Conclusions

In this abstract, we have shown that the theoretical framework of FWM can be effectively extended to take wave conversions into account. By applying the resulting migration algorithm on a model containing a strong reflector we have seen that elastic FWM outperforms conventional, acoustic FWM in a case where strong wave-conversion effects are present. While these results are promising, but not perfect, the main limitations of the method are due to the limitations of Shuey’s approximation. Moving forward,

we therefore recommend examining alternatives to Shuey's approximation which more closely match the true reflection and transmission coefficients at larger angles of incidence.

Acknowledgements

The members of the Delphi consortium are thanked for their support of this research.

References

- Berkhout, A.J. [2014a] Review Paper: An outlook on the future of seismic imaging, Part I: forward and reverse modelling. *Geophysical Prospecting*, **62**(5), 911–930.
- Berkhout, A.J. [2014b] Review Paper: An outlook on the future of seismic imaging, Part II: Full-Wavefield Migration. *Geophysical Prospecting*, **62**(5), 931–949.
- Berkhout, A.J. [2014c] Review Paper: An outlook on the future of seismic imaging, Part III: Joint Migration Inversion. *Geophysical Prospecting*, **62**(5), 950–971.
- Ensley, R.A. [1984] Comparison of *P*- and *S*-wave seismic data: A new method for detecting gas reservoirs. *GEOPHYSICS*, **49**(9), 1420–1431.
- Jones, I.F. and Davison, I. [2014] Seismic imaging in and around salt bodies. *Interpretation*, **2**(4), SL1–SL20.
- Kennett, B.L.N. [1984] AN OPERATOR APPROACH TO FORWARD MODELING, DATA PROCESSING AND MIGRATION. *Geophysical Prospecting*, **32**(6), 1074–1090.
- Shuey, R.T. [1985] A simplification of the Zoeppritz equations. *GEOPHYSICS*, **50**(4), 609–614.
- Virieux, J. and Operto, S. [2009] An overview of full-waveform inversion in exploration geophysics. *GEOPHYSICS*, **74**(6), WCC1–WCC26.

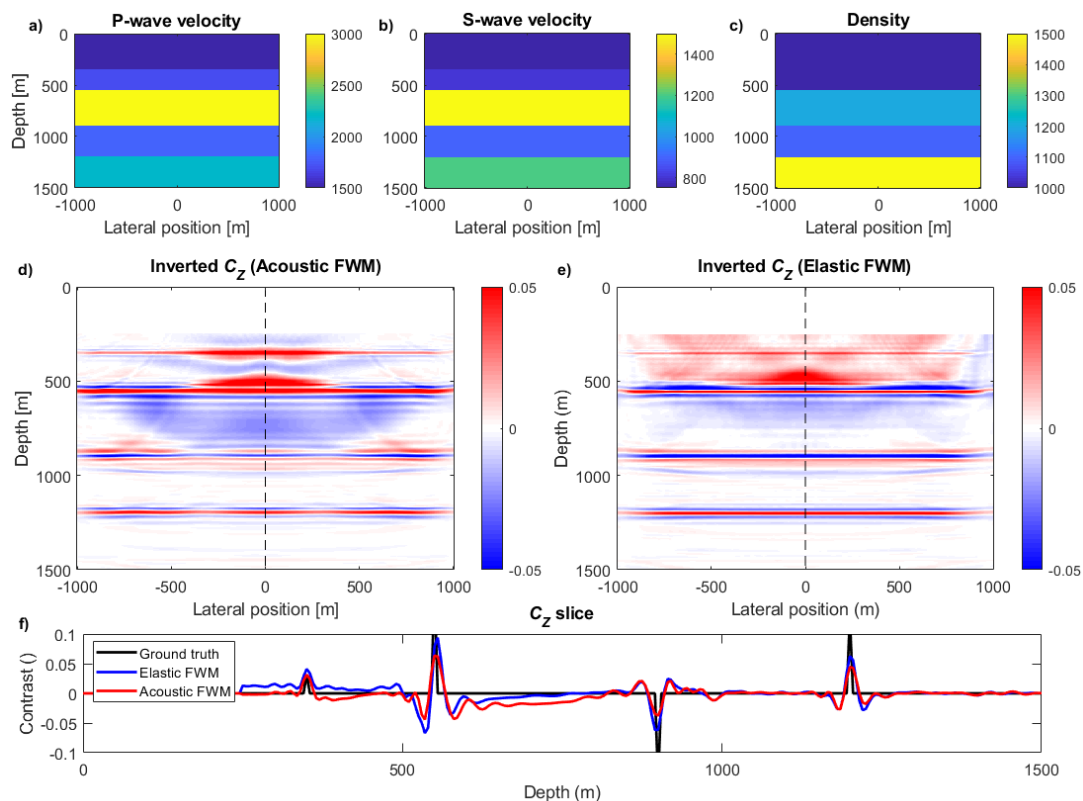


Figure 1 Comparison of acoustic and elastic FWM. The ground-truth *P*-wave velocity, *S*-wave velocity and density profiles are shown in figures (a), (b) and (c), respectively. Figures (d) and (e) show the zero-incidence reflectivity $C_z = (C_p + C_\rho) / 2$ for acoustic FWM and elastic FWM, respectively. Finally, figure (f) shows a slice through the centre of figures (d) and (e).